Solid State Communications, Vol.61,No,8, pp.487-489, 1987.
Printed in Great Britain.

0038-1098/87 $3.00 + .00
Pergamon Journals Ltd.

INTERFERENCE EFFECTS OF RAMAN SCATTERING BY LO-PHONONS NEAR THE $E_0+\Delta_0$-GAP STUDIED ON $(\bar{1}\bar{1}\bar{3})$, (111), AND $(\bar{1}\bar{1}\bar{1})$ FACES OF GaAs

W. Kauschke, V. Vorlicek*, M. Cardona,

Max-Planck-Institut für Festkörperforschung,
Heisenbergstraße 1, D-7000 Stuttgart 80,
Federal Republic of Germany,

L. Viña, and W.I. Wang

IBM Thomas J. Watson Center, Yorktown Heights, N.Y. 10598,
U. S. A.

Received November 20, 1986 by M. Cardona

We have studied the interference of dipole-allowed deformation-potential Raman scattering and dipole-forbidden Fröhlich-induced scattering by LO-phonons near the $E_0+\Delta_0$-gap on the $(\bar{1}\bar{1}\bar{3})$ face of MBE-GaAs and on the (111) and $(\bar{1}\bar{1}\bar{1})$ faces of bulk GaAs at 100 K. Absolute values of the squared Raman tensor are displayed. A fit of the resonance profile reveals that the purity of the MBE-sample under investigation compares well with that of (001) LPE-samples studied previously. The (111) and $(\bar{1}\bar{1}\bar{1})$ faces of GaAs show opposite signs in the interference, in accordance with symmetry considerations.

Introduction

The interference of dipole-allowed deformation-potential induced and dipole-forbidden Fröhlich-interaction induced Raman scattering by LO-phonons near the $E_0+\Delta_0$-gap is a well established phenomenon in the III-V compounds. It has been observed on the (001) faces of high-purity liquid-phase epitaxial (LPE) GaAs[1,2] and $Al_xGa_{1-x}As$,[3] of metal-organic vapour deposited (MOCVD) InP,[4] and of bulk Czochralski grown GaAs[2] and GaSb[5]. Three different scattering mechanisms for LO-phonons are operative near the $E_0+\Delta_0$-gap. The deformation-potential scattering obeys usual dipole-selection rules (dipole-allowed) and resonates only weakly near $E_0+\Delta_0$, since only three-band terms are operative at the gap. The intrinsic dipole-forbidden Raman scattering arises from the $\vec{q}$-dependence of the intraband matrix elements of the Fröhlich interaction. The third mechanism, also dipole-forbidden, invokes the elastic scattering by ionized impurities, in addition to the Fröhlich electron-phonon interaction. For the third process the momentum conservation is relaxed and LO-phonons of the whole phonon branch can be activated. Both dipole-forbidden scattering mechanisms resonate at all direct gaps. They are described by diagonal Raman tensors and their contributions cannot be separated in a single experiment. The $\vec{q}$-dependent Fröhlich forbidden Raman scattering and the deformation-potential mechanism are, however, mutually coherent and may interfere, whereas the impurity-induced one is incoherent with both. Therefore, a quantitative analysis of the interference of Raman scattering by LO-phonons gives information on the purity of the sample.[2-5]

Experimental

The epitaxial GaAs samples studied were grown on a $(\bar{1}\bar{1}\bar{3})$ oriented semiinsulating substrate by molecular-beam epitaxy. The ionized impurity concentration N_D-N_A was determined from Hall mobility measurements. At 77 K it amounts to $2\cdot10^{15}$ cm^{-3} (μ_{77} = 43000 cm^2/Vs). The (111) and $(\bar{1}\bar{1}\bar{1})$ oriented samples were obtained form Czochralski-grown semiinsulating GaAs with $N_D-N_A \leq 10^{16}$ cm^{-3} in the following way: the ingot was cut in the (111) plane and two opposite surfaces were mechanically polished. For the crystal axes notation we refer to Ref. 2: the Ga-atom is taken to be at the origin and the As-atom at the $(a_0/4)(1,1,1)$ site. We further denote by y', z', x", and z" the vectors $1/\sqrt{2}$ $(1,\bar{1},0)$, $1/\sqrt{3}$ $(\bar{1},\bar{1},\bar{1})$, $1/\sqrt{22}$ $(\bar{3},\bar{3},2)$, and $1/\sqrt{11}$ (1,1,3), respectively. The Raman tensor for dipole-forbidden Raman scattering by LO-phonons remains diagonal in all coordinate systems. The squared Raman polarizability $|a_{FI}|^2$ for impurity-induced scattering by LO-phonons is given by Eq. (A1) of Ref. 2. Equations (15) and (16) of Ref. 2 display the expressions for the Raman polarizability a_F of intrinsic $\vec{q}$-dependent scattering as a function of wavevector $\vec{q}$ and of excitation energy $\hbar\omega_L$. With the convention of Ref. 2, Eq. (15) includes in the Fröhlich constant C_F a sign which reverses for backscattering at opposite surface. We chose the sign of a_F as in Ref. 2 ($C_F > 0$). Then a_F must be replaced by $-a_F$, when going from a (001) face to a $(00\bar{1})$ face, from a (111) to a $(\bar{1}\bar{1}\bar{1})$ face, or from a (113) face to a $(\bar{1}\bar{1}\bar{3})$ face.

*On leave from: Institute of Physics, Czechoslovak Academy of Sciences, Prague, Czechoslovakia.

For deformation- potential scattering by LO-phonons the Raman tensor has to be written as an appropriate linear combination of the three basis tensors referred to the crystallographic axes. The result for backscattering at the different faces used here can be summarized as follows (referred to the crystallographic axes):

$$\overleftrightarrow{R}_{DP,z'} = \frac{1}{\sqrt{3}}\begin{pmatrix} 0 & a_{DP} & a_{DP} \\ a_{DP} & 0 & a_{DP} \\ a_{DP} & a_{DP} & 0 \end{pmatrix}, \quad (1)$$

$$\overleftrightarrow{R}_{DP,\bar{z}'} = \overleftrightarrow{R}_{DP,z'}, \quad (2)$$

$$\overleftrightarrow{R}_{DP,z''} = \frac{1}{\sqrt{11}}\begin{pmatrix} 0 & 3a_{DP} & a_{DP} \\ 3a_{DP} & 0 & a_{DP} \\ a_{DP} & a_{DP} & 0 \end{pmatrix}, \text{ and} \quad (3)$$

$$\overleftrightarrow{R}_{DP,\bar{z}''} = \overleftrightarrow{R}_{DP,z''}. \quad (4)$$

The expression of the Raman polarizability a_{DP} as a function of the parameters of the critical points E_o-$E_o+\Delta_o$, E_1-$E_1+\Delta_1$, and higher gaps is given by Eq. (4) of Ref. 4. We measured in four different backscattering configurations with polarization $\hat{e}_S \| \hat{e}_L$ which correspond to the following squared Raman tensors:

- on a $(\bar{1}\bar{1}\bar{3})$ face

I. $z''(y',y')\hat{\bar{z}}''$ $\left|-a_F+\frac{3}{\sqrt{11}}a_{DP}\right|^2+\left|a_{Fi}\right|^2$, (5)

II. $z''(x'',x'')\hat{\bar{z}}''$ $\left|-a_F+\frac{15}{11\sqrt{11}}a_{DP}\right|^2+\left|a_{Fi}\right|^2$, (6)

- on a (111) face

III. $z'(y',y')\hat{\bar{z}}'$ $\left|+a_F-\frac{1}{\sqrt{3}}a_{DP}\right|^2+\left|a_{Fi}\right|^2$, and (7)

- on a $(\bar{1}\bar{1}\bar{1})$ face

IV. $\hat{\bar{z}}'(y',y')z'$ $\left|-a_F-\frac{1}{\sqrt{3}}a_{DP}\right|^2+\left|a_{Fi}\right|^2$. (8)

It is worthwile to note that the squared Raman tensor for backscattering at a (113) face with $\hat{e}_S \| \hat{e}_L$ are obtained from Eqs. (5) and (6) by replacing a_F by $-a_F$.

Absolute squared Raman tensors were determined by the sample substitution method using high purity silicon as a reference.[6] The corrections for absorption, reflectivity, and refractive index of GaAs and Si are the same as described in Refs. 2 and 5. The measurements were performed at liquid nitrogen temperature with a cw dye laser operated with the dye DCM (Lambda Physik, Göttingen).

Results and Discussion

Figure 1 shows the results obtained on a $(\bar{1}\bar{1}\bar{3})$ face of MBE-GaAs in terms of squared Raman polarizabilities. The points represent experimental data, whereas the lines are calculated with a_F, a_{Fi}, and a_{DP} as determined from the interference curves of a (001) LPE-GaAs sample at 100 K (μ_{77} = 100000 cm^2/Vs, $N_D-N_A \le 10^{13}$ cm^{-3}).[3]

The ratio of intrinsic and extrinsic dipole-forbidden Raman scattering efficiencies $|a_F|^2/|a_{Fi}|^2$ amounts to 0.63. The agreement of the curves with the experimental data on MBE-GaAs is excellent, especially for the solid line (constructive interference, configuration I). Some discrepancies are seen at the dashed line (destructive interference, configuration II), which may be due to a larger experimental error because of lower scattering efficiencies in this configuration and to some deviation from the ideal $(\bar{1}\bar{1}\bar{3})$ orientation. A higher amount of impurity-induced dipole-forbidden scattering would improve the agreement for the dashed line, however, it would worsen the fit of the solid line. We, hence, suggest that the purity of the MBE-samples studied is similar to that of LPE-samples.

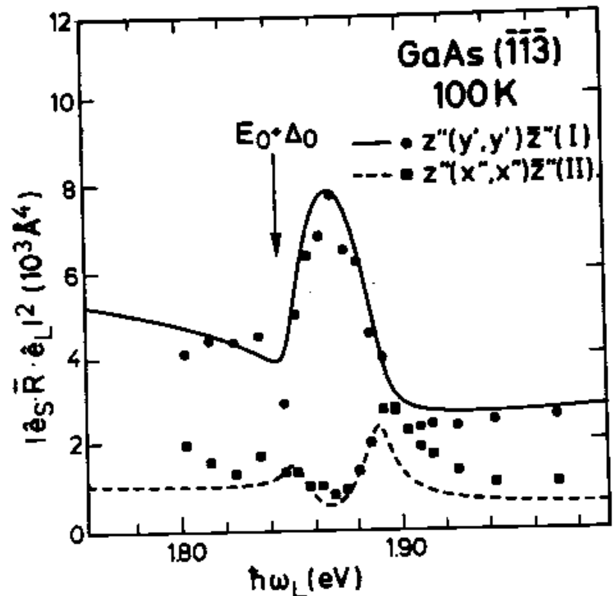

Fig. 1: Squared Raman polarizabilities for scattering by one LO-phonon measured on GaAs $(\bar{1}\bar{1}\bar{3})$ with $\hat{e}_L \| \hat{e}_S$. The lines correspond to a fit as described in the text.

Figure 2 depicts the result of calculation for a (113) face with the same parameters as used for the curves of Fig. 1. The resonance profiles from this face reveal interferences opposite to those for the $(\bar{1}\bar{1}\bar{3})$ face. The measurements of LO-phonon interference effects thus enables to distinguish easily between opposite faces in a non-destructive way.

This fact is demonstrated in Fig. 3 for {111} faces of bulk semiinsulating GaAs. The (111) face behaves differently from the $(\bar{1}\bar{1}\bar{1})$ face over the spectral range under investigation. Also, different electrical behavior is expected for these two faces due to different surface states.[7,8] Undoubtedly, the interference pattern is obscured by a broadening and a large amount of impurity-induced Raman scattering. The maximum resonant enhancement of LO-phonon scattering occurs in both samples at different energies. The resonance maximum for the $(\bar{1}\bar{1}\bar{1})$ face is situated near the gap plus half of the LO-phonon energy ($E_o+\Delta_o+\hbar\Omega_{LO}/2$), as it is usually the case for

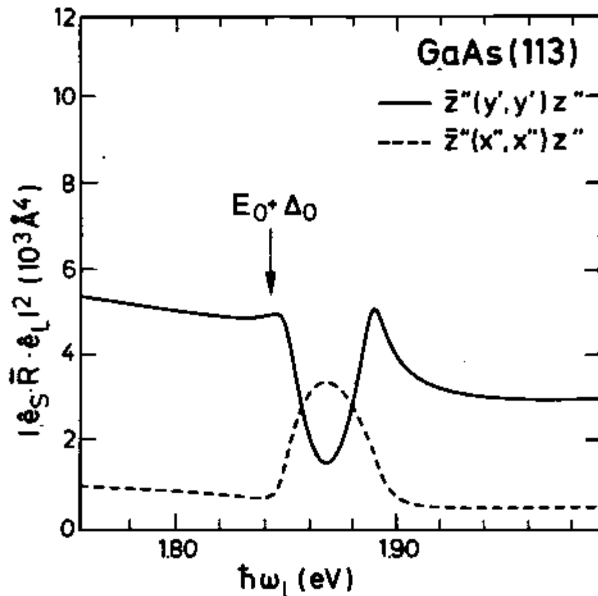

Fig. 2: Calculated interference curves for backscattering at a (113) face of GaAs with $\hat{e}_L \| \hat{e}_S$.

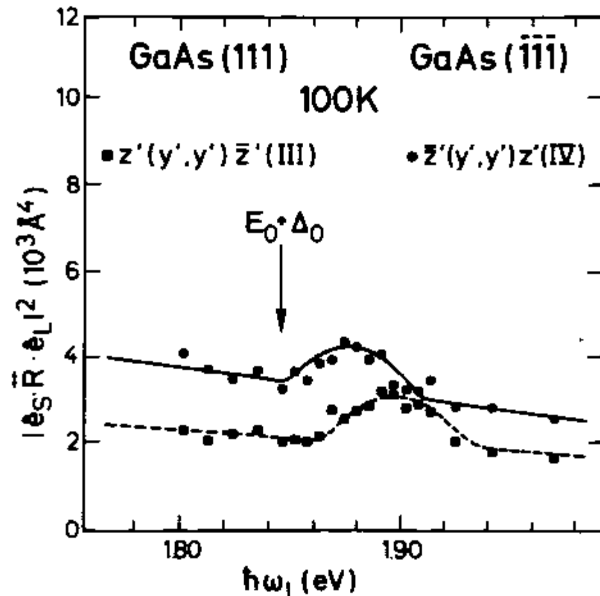

Fig. 3: Squared Raman polarizabilities for scattering by one LO-phonon measured on (111) and ($\bar{1}\bar{1}\bar{1}$) faces of GaAs with $\hat{e}_L \| \hat{e}_S$. The lines are drawn as a guide to the eye.

constructive interference. On the other hand, the (111) face reveals its maximum enhancement near $E_o+\Delta_o+\hbar\Omega_{LO}$, as expected for outgoing resonance and destructive interference.

In conclusion, we have demonstrated that the interference of dipole-allowed and dipole-forbidden scattering can be observed on different sample faces. The measurements constitute a non-destructive method allowing to distinguish the (ijk) face from the ($\bar{i}\bar{j}\bar{k}$) one in polar semiconductors, in addition to distinguish the [1,1,0] direction from [1,$\bar{1}$,0].

Acknowledgement

The authors express their gratitude to H. Hirt, M. Siemers, and P. Wurster for technical assistance. One of us (V.V.) thanks the Max-Planck-Gesellschaft for the financial support.

References

1. J. Menéndez and M. Cardona, Phys. Rev. Lett. 51, 1297 (1983).
2. J. Menéndez and M. Cardona, Phys. Rev. B 31, 3696 (1985).
3. W. Kauschke, M. Cardona, and E. Bauser, unpublished.
4. W. Kauschke and M. Cardona, Phys. Rev. B 33, 5473 (1986).
5. W. Kauschke and M. Cardona, unpublished.
6. M. Cardona, Light Scattering in Solids II, Vol. 50 of Topics in Applied Physics, edited by M. Cardona and G. Güntherodt, (Springer, Berlin, 1982), p. 19.
7. C.A. Mead and W.G. Spitzer, Phys. Rev. 134, A713 (1964).
8. S. Buchner, L.Y. Ching, and E. Burstein, Phys. Rev. B 14, 4459 (1976).